

# Ku-band Antenna Array Element Based on Fabry-Perot Cavity

A. M. Alexandrin, S. V. Polenga<sup>1</sup>, A. V. Stankovsky, A. D. Nemshon, Y. A. Litinskaya, A. D. Hudonogova, Yu. P. Salomatov

*Institute of Engineering Physics and Radioelectronics  
Siberian Federal University  
660074, Kirensky street 28, Krasnoyarsk, Russia  
<sup>1</sup>twinlive@gmail.com*

The results of simulation and experimental study of the Ku-band antenna array element based on Fabry-Perot cavity (FPC) are presented in the article. The FPC is implemented as double-layered subwavelength FSS acting as partially reflecting surface (PRS). The matching element in form of a dielectric pyramid is presented. The reflection coefficient of fabricated prototype is below  $-10$  dB within the operating frequency band. The gain of the prototype exceeds  $18.7$  dBi within a range of  $12$ – $12.7$  GHz. The frequency band at  $-3$  dB from maximum gain level is  $9\%$ . The presented array element can be used in high efficient arrays for satellite communications and television.

## I. INTRODUCTION

The Fabry-Perot cavity (FPC) is a main kind of the optical resonators which consists of two parallel mirrors turned to each other so that a resonant optical standing wave can form between them. One of the mirrors is usually made partially transparent for taking out the radiation in one primary direction.

In the past decades this principle was actively studied for using in radio frequency band [1–4]. It allows constructing highly effective and technologically simple radiators. This article focuses on the development of array element based on FPC. The frequency band of  $12$ – $12.7$  GHz was chosen for possible applications in satellite communication systems.

## II. UNIT CELL

For the occurrence of a resonance in FPC it's necessary that an electric distance between two flat parallel mirrors was equal to  $\lambda/2 + n\lambda$ , where  $n$  is any natural number including  $0$ . However in this case the condition for the resonance is met only at single frequency, so the whole system is narrowband. For satisfying the resonance conditions in a wide frequency band it's necessary that at least one of the reflectors had a positive slope of the phase of reflected wave [1] (see fig. 2, reference curve). Such behaviour of the phase allows to compensate the wavelength change and maintain constant electric distance of  $\lambda/2$  between the reflectors. One of methods of constructing the partially reflective surface (PRS) is the use of frequency selective surface (FSS). The double-layered element of such FSS acting as PRS is presented on fig. 1.

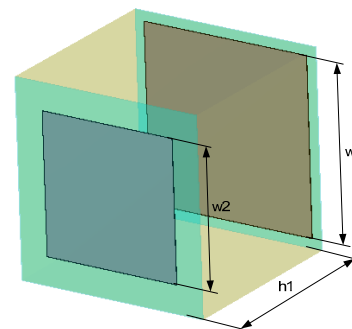


Figure 1. Unit cell

The PRS cell contains two layers of subwavelength microstrip patches and a dielectric layer with  $\epsilon = 1.05$  between them. The cell parameters are  $h_1 = 12.7$  mm,  $w_2 = 9.5$  mm,  $w_1$  being a variable parameter.

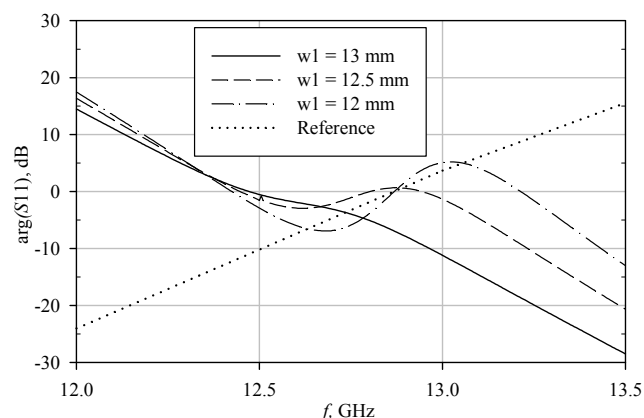


Figure 2. Phase of reflection coefficients of PRS unit cell

The reflected wave phase of this cell has a bend at the resonance frequency (fig. 2, 3) thus providing a positive slope within a limited band. Fig. 2 presents the curves for three different sizes of a patch in the first layer  $w_1$ . With decreasing  $w_1$  the phase of reflected wave approaches the reference curve in a wider frequency band but the module of reflection coefficient significantly decreases.

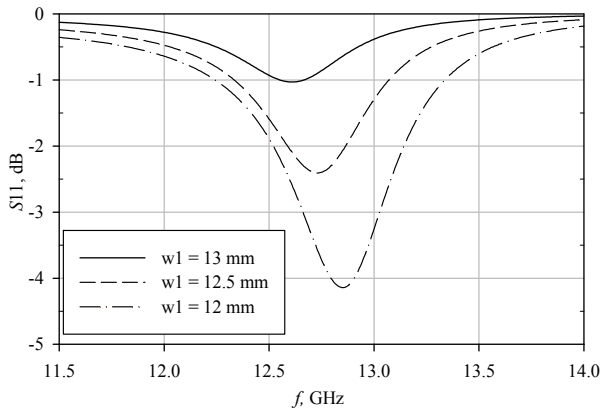


Figure 3. Reflection coefficients of PRS unit cell

### III. FPC ANTENNA ARRAY ELEMENT

For maintaining low profile of antenna system it's necessary to choose the minimum distance between mirrors equal to  $\lambda/2$ . The criterion for such choice is maximum aperture efficiency, not maximum gain because this element is planned to be used as an array element. The resonator CAD model is shown on fig. 4.

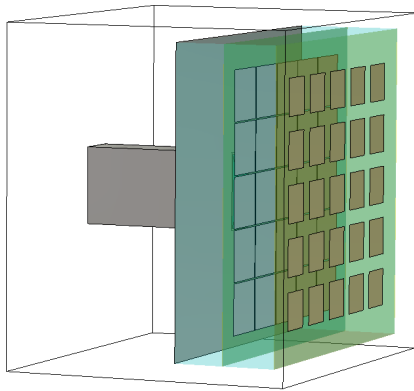


Figure 4. Fabry Perot cavity CAD model

The open waveguide with matching dielectric pyramid is used as feeder (fig. 5).

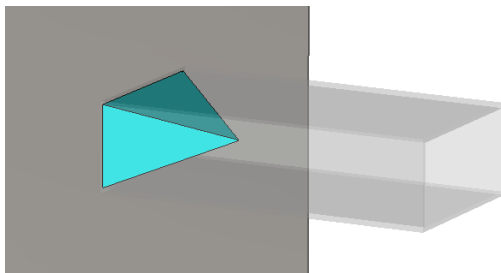


Figure 5. Matching pyramid

It's known that matching is the weak point of FBC so that additional auxiliary elements are required for this purpose. In our case the dielectric pyramid made from PTFE ( $\epsilon = 2.1$ ) was introduced to allow broadband matching (Fig. 6)

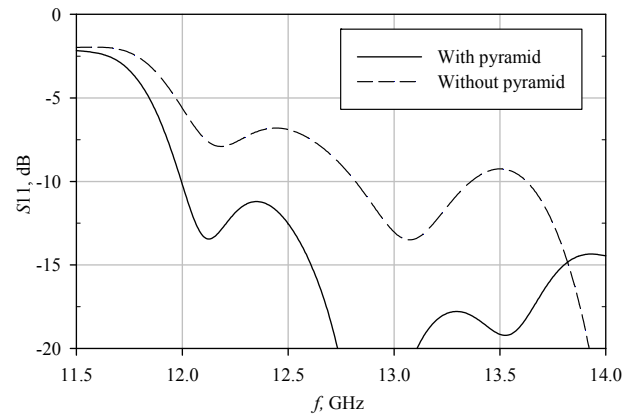


Figure 6. Reflection coefficient of FPC with and without matching element

The gain for different values of  $w_1$  is shown on fig. 7.

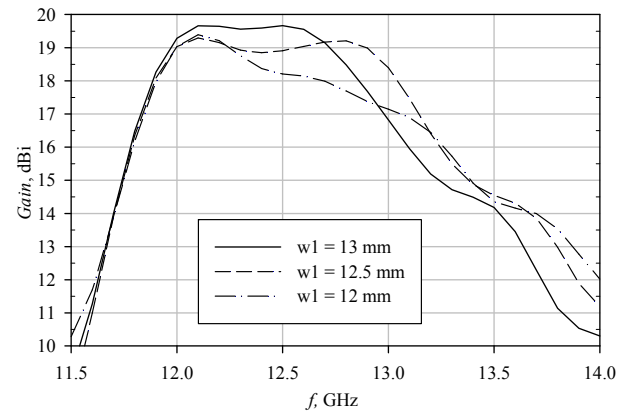


Figure 7. FPC realized gain

At decreasing  $w_1$  from 13 mm to 12.5 mm the frequency band widens and gain decreases. This means that electrical distance between the reflectors remains the same in wider range of frequencies (the ascendant sector of reflection phase in fig. 2). However, with further decreasing of  $w_1$  the reflection coefficient of PRS significantly decreases (fig. 3), deteriorating the efficiency of resonator functioning. The gain decrease is also connected with increased reflections from the input port (fig. 8).

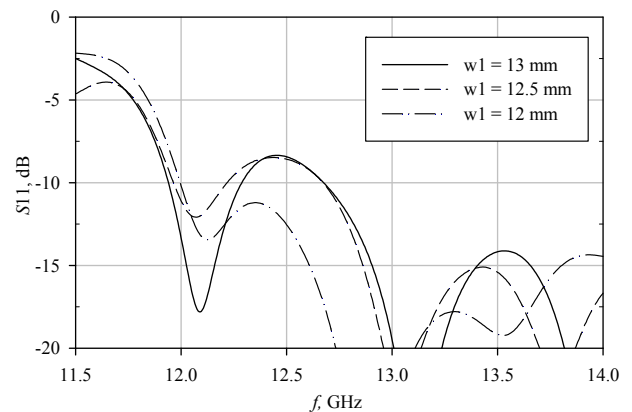


Figure 8. Reflection coefficient of FPC

Despite the fact that decreasing of  $w_1$  leads to decreasing of PRS reflection coefficient, reflections from the whole resonator increase in operating frequency range.

For fabrication purpose the value of  $w_1$  was chosen to be 13 mm.

#### IV. FPC MANUFACTURING AND MEASUREMENT

The topology of FPC is made on metallized PET sheet of 0.15 mm thickness by the photolithography method. The back screen is made of galvanized steel. The standard WR-75 waveguide-to-coaxial transition was used as a feeder. The expanded polystyrene with  $\epsilon = 1.05$  was used as filling between layers. All the structure elements are shown on fig. 9.

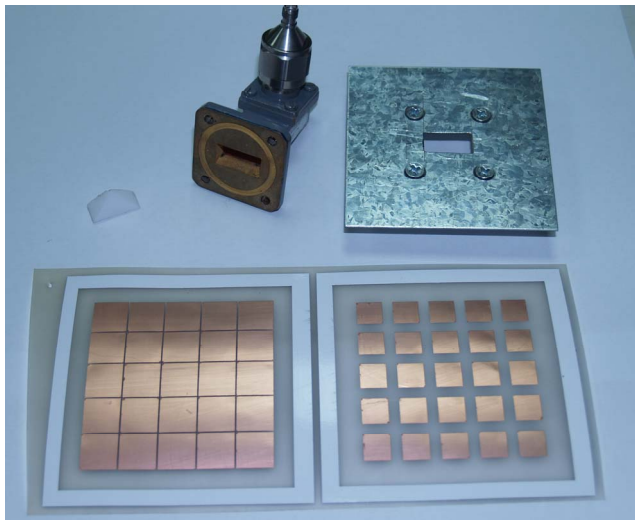


Figure 9. Elements of FPC structure

The resonator elements are assembled with double-sided adhesive tape. The dimensions of the resonator are  $80 \times 80 \times 27$  mm not including the waveguide transition.

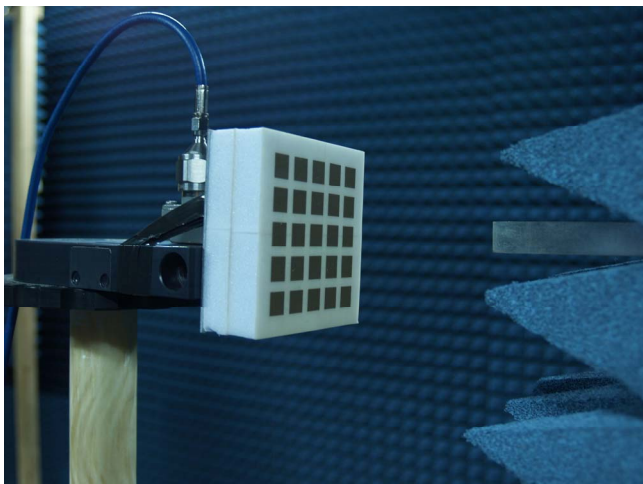


Figure 10. Near field measurements in anechoic chamber

The measurements were carried out in an anechoic chamber by the near field scanning method [5] (fig. 10). The amplitude and phase distributions of the FPS prototype on highest and lowest frequencies of operating band are shown on fig. 11.

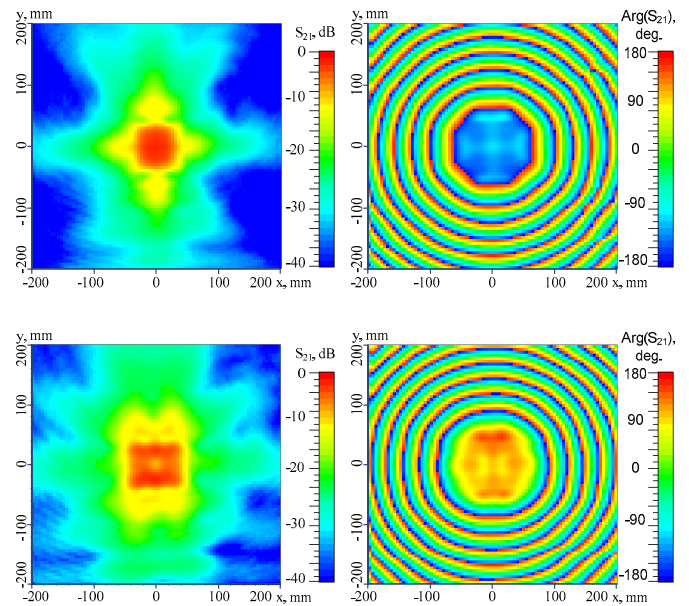


Figure 11. Amplitude and phase distributions: top - 12 GHz; bottom - 12.7 GHz

The y-axis corresponds to electric field vector direction. The amplitude distribution in antenna aperture is close to uniform in all frequency range. With the frequency increase, widening of the high amplitude region occurs in  $H$ -plane. The phase distribution is close to uniform, phase errors not exceeding  $45^\circ$  within the high amplitude region.

The amplitude radiation patterns are presented on fig. 12—15. It should be mentioned that the measurement method used has high accuracy within a limited range of angles ( $\pm 60^\circ$ ). Thereby the divergence between calculated and measured patterns at large angles ( $>60^\circ$ ) is connected with measurement method limitations.

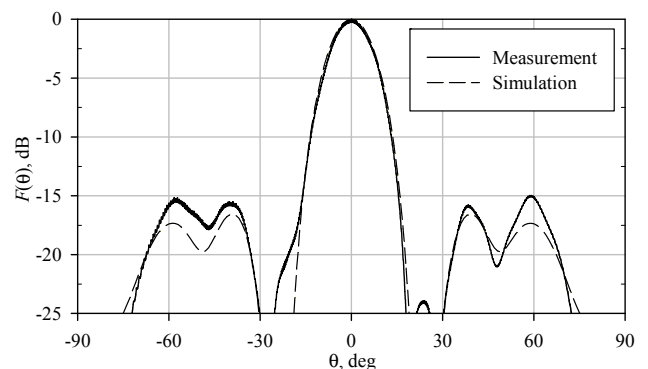


Figure 12. Radiation pattern at 12 GHz in  $E$ -plane

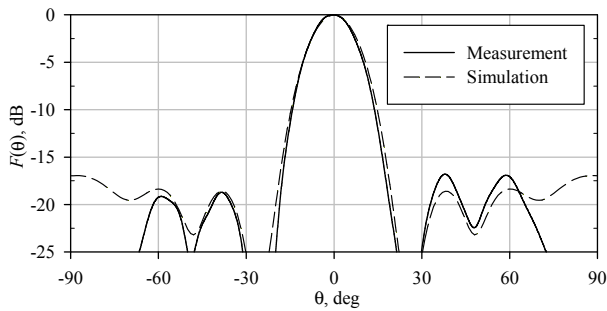


Figure 13. Radiation pattern at 12 GHz in  $H$ -plane

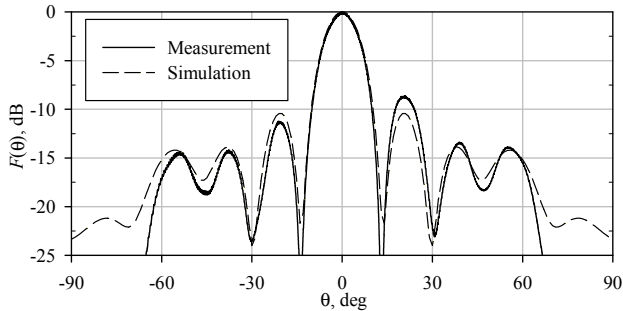


Figure 14. Radiation pattern at 12.7 GHz in  $E$ -plane

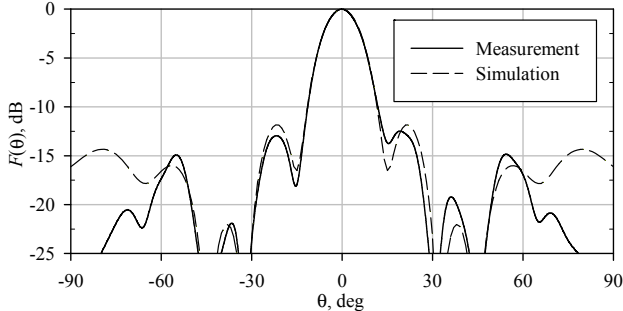


Figure 15. Radiation pattern at 12.7 GHz in  $H$ -plane

At 12.7 GHz high side lobe level in  $E$ -plane is observed due to some notch on the amplitude distribution. In total the measured and the calculated results demonstrate good agreement with the deviations being connected partially with manufacturing errors and losses not concerned and partially with the measurement method limitations.

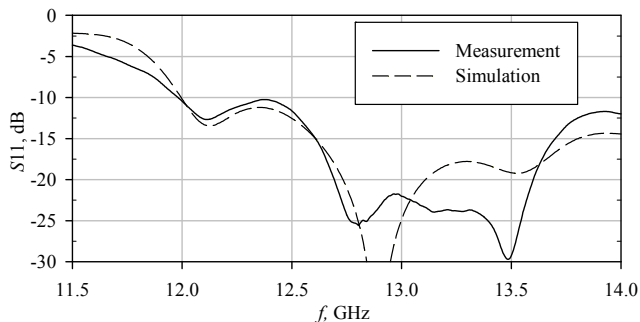


Figure 16. FPC model reflecting coefficient

The calculated and measured reflection coefficient values have good agreement (fig 16). An increased level of

reflections within the frequency range is due to reflections from waveguide transition, not considered in simulation.

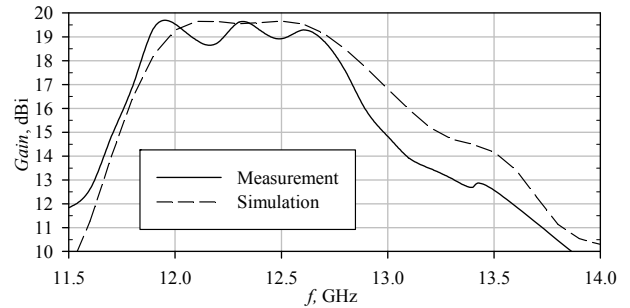


Figure 17. FPC gain

The measured gain of the prototype was 0.5 dB lower than was calculated. In total the measured curve closely corresponds to the calculated one, the difference being possibly due to the losses in resonator material. An additional study was carried out with galvanized steel screen being replaced by the copper screen, but this didn't affect the FPC characteristics.

## V. CONCLUSION

The article presents the results of simulation and measurement of the FPC based array element. The influence of changing parameters of subwavelength FSS on the PRS and the whole resonator characteristics is reviewed. The introduction of matching element in the form of pyramid allowed to reduce the reflections to the acceptable level of  $-10$  dB. The gain was 0.5 dB lower than that simulated which can possibly be connected with the losses in materials or with the measuring antenna gain errors.

The FPC based element can be used as an array element for the ground satellite terminals.

## ACKNOWLEDGMENT

The publication is supported by Krasnoyarsk Region Science and Technology Support Fund.

## REFERENCES

- [1] Y. Ge, K. P. Esselle and T. S. Bird, "The Use of Simple Thin Partially Reflective Surfaces With Positive Reflection Phase Gradients to Design Wideband, Low-Profile EBG Resonator Antennas," in *IEEE Transactions on Antennas and Propagation*, vol. 60, no. 2, pp. 743-750, Feb. 2012.
- [2] K. Konstantinidis; A. P. Feresidis; P. S. Hall, "Multilayer partially reflective surfaces for broadband Fabry-Pérot cavity antennas," *IEEE Transactions on Antennas and Propagation*, vol. 62, pp. 3474-3481, 2014.
- [3] Y. Sun; Z. Ning Chen; Y. Zhang; H. Chen; Terence S. P. See, "Subwavelength substrate-integrated Fabry-Pérot cavity antennas using artificial magnetic conductor," *IEEE Transactions on Antennas and Propagation*, vol. 60, pp. 30-35, 2012.
- [4] Avinash R. Vaidya; Rajiv K. Gupta; Sanjeev K. Mishra; Jayanta Mukherjee, "Effect of superstrate height on gain of MSA fed Fabry Perot cavity antenna," *Antennas and Propagation Conference (LAPC)*, 2011.
- [5] A. S. Ivanov, K. V. Lemberg, S. V. Polenga, R. M. Krylov and Y. P. Salomatov, "Implementation of antenna near-field scanning without using probe position sensors," *Control and Communications (SIBCON), 2015 International Siberian Conference on*, Omsk, 2015, pp. 1-3.